Reliability analysis of deep pressurized tunnels excavated in the rock mass with rheological behavior

Transportation Geotechnics 45 (2024) 101212

Contents lists available at ScienceDirect

Transportation Geotechnics

journal homepage: www.elsevier.com/locate/trgeo

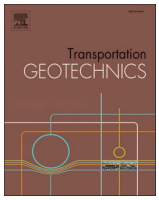

Reliability analysis of deep pressurized tunnels excavated in the rock mass with rheological behavior

Milad Zaheri [a], Masoud Ranjbarnia [a,b], Pierpaolo Oreste. [c,*]

[a] Department of Geotechnical Engineering, Faculty of Civil Engineering, University of Tabriz, Tabriz, Iran
[b] Institute of Geoscience, Christian-Albrecht's-University of Kiel, Germany
[c] Department of Environmental, Land and Infrastructure Engineering, Politecnico di Torino, Turin, Italy

ARTICLE INFO

Keywords:
Pressurized tunnels, probabilistic analysis, time-dependent behavior
Response surface methodology
Tridimensional numerical model
Rheological rock mass
Excavation damaged zone
Monte Carlo Method (MCM)

ABSTRACT

Design of pressurized tunnels in rock masses which have a time-dependent behavior is a challenging task. On the one hand, time-dependent behavior not only imposes extra pressure to the tunnel lining but also leads the rock mass hydraulic conductivity to vary continuously; this aspect can exert another adding pressure to the lining. On the other hand, the uncertainty of the rock mass properties, which can differ from one point to another one, is another source of instability. Furthermore, the excavation method, i.e., poor blasting, which creates a weaker damaged zone around the tunnel, intensifies the complexity of the problem.

This paper presents a probabilistic approach to investigate the influencing factors on the behavior of underwater tunnels. The behavior of the original and damaged rock masses is considered as visco-elastoplastic (using the CVISC model) in order to be able to consider its rheological character. Four parameters including Geological Strength Index (GSI), rock mass permeability, thickness of the damaged zone, and Kelvin shear modulus, which showed the most influencing effects in a developed sensitive analysis, were chosen as random variables. The Monte Carlo Method (MCM) was used to generate random values for these variables, adopting the normal distribution. Then, the response surface methodology (RSM) was used to intelligently lessen the number of generated values, and then to prepare datasets with the inclusion of all variables. The calculations were carried out for each provided dataset by a tridimensional numerical model ($FLAC^{3D}$ code) to obtain the tunnel wall displacement and the lining pressure, over time, as the results of the calculation. The RSM is again employed to obtain the relationships between inputs and output values and finally to have the probability function of the outputs.

The results show that a right-skewed Gamma distribution governs the outputs: i.e. the distribution mass is concentrated on the left side of the probability distribution. Furthermore, when the water pressure is enhanced, the skewness of the probability distribution for the tunnel wall convergence and the lining pressure increases and decreases, respectively. Finally, it was possible to detect how the designing of pressurized tunnels using a deterministic approach, which adopts a unique value for the input parameters, may be misleading when the internal water pressures are high.

Introduction

Tunneling in soft rock masses located at highly stress conditions is a challenging task [6,13,32,34]. It causes the rock masses to experience a time-dependent behavior, which may cause a tunnel failure over time. This behavior is of great interest as it has been one of the main reasons of tunnel collapse.

Wang et al. [26] incorporated the growth of the tunnel radius from zero to a desired value according to a time-dependent function, and studied the response of the tunnel. Nomikos et al. [20] evaluated the induced lining pressure over time for tunnels embedded in soft rocks. Paraskevopoulou and Diederichs [21] investigated the role of the excavation method to find unsupported tunnels convergence. Quevedo et al. [22] highlighted the shrinkage and creep behavior of the lining system on the tunnel response excavated in a rheological rock mass. Chu et al. [2,3] investigated the influence of tunneling operation stoppage on tunnels behavior. Do et al. [5] and Zeng et al. [40] evaluated the effect of the sequential installation of two layers of lining on the performance of

* Corresponding author.
E-mail addresses: Miladzaheri@tabrizu.ac.ir (M. Zaheri), M.ranjbarnia@tabrizu.ac.ir (M. Ranjbarnia), Pierpaolo.Oreste@polito.it (P. Oreste.).

https://doi.org/10.1016/j.trgeo.2024.101212
Received 8 November 2023; Received in revised form 2 February 2024; Accepted 8 February 2024
Available online 10 February 2024

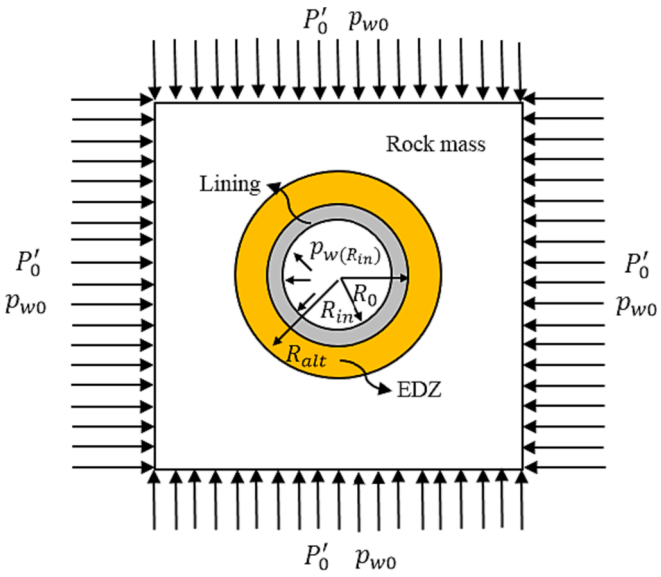

Fig. 1. The geometry of the assumed model.

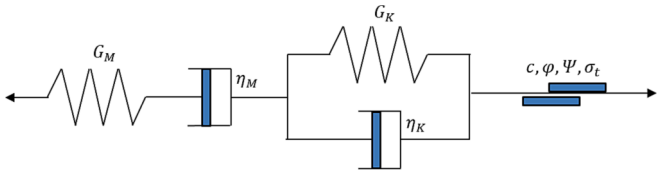

Fig. 2. The elastic-visco plastic (CVISC) model.

deep tunnels in weak rock masses. Kargar and Haghgouei [18] and Wang et al. [28] found the influence of non-hydrostatic in-situ stress on time-dependent behavior. Song et al. [24] used a simulation to obtain the stress and displacement around underground openings considering the sequential installation of two supporting systems. Wang et al. [27] found the stress and displacement distributions around a tunnel with an elliptical cross-section. Wang et al. [25] and Zeng et al. [39] considered a surcharge loading and analyzed the response of circular and non-circular shallow tunnels. Zaheri et al. [33] and Zaheri and Ranjbarnia [30,31] evaluated the role of poor blasting in tunnelling on the so-called Excavation damaged zone (EDZ) and the consequent tunnel long-term response. It was found that it significantly influences the time-dependent displacement of the tunnel because this zone has lower strength and deformation properties than the undamaged zone [12,16,29].

In pressurized tunnels, water seepage which exerts a pressure on the tunnel lining can be a source of instability. It occurs during tunnel excavation in saturated rock masses and after excavation during water transferring. The direction of seepage force can be inward or outward depending on the relative values of the initial pore water pressure (due to the water table) and of the internal water pressure (due to water transferring).

Similar to the time-dependent issue, attempts have been conducted to investigate the role of water seepage on tunnel behavior. Brown and Bray [1] found the seepage force effect on the underwater tunnel resting on an elastoplastic rock mass. They considered variable permeability coefficients for the rock mass in the induced plastic zone around the tunnel. Zareifard and Fahimifar [36] obtained the induced lining pressure and the corresponding tunnel displacement, due to the water seepage in a rock mass with constant permeability. In other works, Fahimifar et al. [9–11] used the model by Huangfu et al. [17] for the pore pressure distribution around tunnels, and obtained the distribution of displacements and stresses in the ground. Kolymbas and Wagner [19] assumed a non-radial direction of seepage force toward the tunnel, and Fahimifar and Zareifard [7,8] and Zou and Li [41] used this model and found the tunnel wall convergence. As the poor blasting creates new cracks and amplifies the existing ones, the hydraulic conductivity of the *EDZ* is greater; this phenomenon causes the seepage force to be different from that in the undisturbed rock mass. Zareifard and Fahimifar [37] and Zareifard and Shekari [38] investigated the effects of poor blasting of tunnels on the value of the seepage force.

Most of the studies in the case of pressurized tunnels refer to the short-term behavior. Recently, Zaheri et al. [35] theoretically modeled this type of tunnels in the rock mass with a Burger visco-elastic behavior. In this effort, they considered the interaction between the time-dependent properties and the hydraulic conductivity of the rock mass. It was found that seepage forces on the tunnel lining significantly differ over time. Since the squeezing condition causes the rock mass around the tunnel to be more softened over time, it leads the hydraulic conductivity to change. Hence, the seepage force alters over time: it means also a change in the tunnel convergence.

Reviewing the previous researches shows that there is a lack of studies regarding the long-term behavior of pressurized tunnels. Therefore, some aspects involving the role of different parameters pertaining to the time-dependent behavior and of the hydraulic conductivity particularly when considering the EDZ presence around the tunnel (due to a poor blast-induced damage), have not yet been explored. The blast-induced damage leads to the formation of a poor zone around the tunnel, which increases the hydraulic conductivity of the rock mass, resulting in elevated pressure on the tunnel lining. The variability of this pressure over time can pose critical challenges to the long-term stability of the tunnel.

This study uses a probabilistic approach, as it considers the inherent uncertainty of the rock mass properties. Because, it provides a quantitative tool for making engineering judgments in projects. It shows how uncertainties of a parameter affect safety, and causes our decision-making process more clearly.

A parametric study is initially performed to investigate the effect of different geo-mechanical parameters; then a probabilistic distribution is assigned to the most influencing ones. The Monte Carlo Method (MCM) is used to generate a large number of random values for the rock mass parameters. The response surface methodology (RSM) is then employed to lessen the number of generated values. The analyses in terms of random values are performed by the FLAC^{3D} numerical code (which makes possible to assign visco plastic constitutive behavior to the rock mass) to obtain the outputs i.e., the lining stress and the tunnel convergence over time. Finally, the probability distributions of outputs are calculated and commented.

Problem definition and assumptions

A circular tunnel is excavated in a saturated rock mass with a rheological behavior. The excavation method by adopting uncontrolled blasting may lead the rock mass around the tunnel to a damage, and thus, to induce the so-called “Excavation Damaged Zone (*EDZ*)”. This zone has lower mechanical properties and a higher hydraulic conductivity than the undamaged rock mass (see Fig. 1).

The behavior of the damaged and undamaged rock masses is considered of elastic-visco plastic type, known as the CVISC model; it is a combination of the Burgers model and the Mohr-Coulomb strength criterion combined in series (Fig. 2).

As noticed, six independent parameters are required to predict the behavior of rock masses in these zones. They are:

- Kelvin and Maxwell viscosities (η_K, η_M),
- Kelvin and Maxwell shear moduli (G_k, G_M) and
- Rock mass strength parameters (friction angle (φ) and cohesion (c)).

The strength parameters and the Maxwell shear modulus of rock

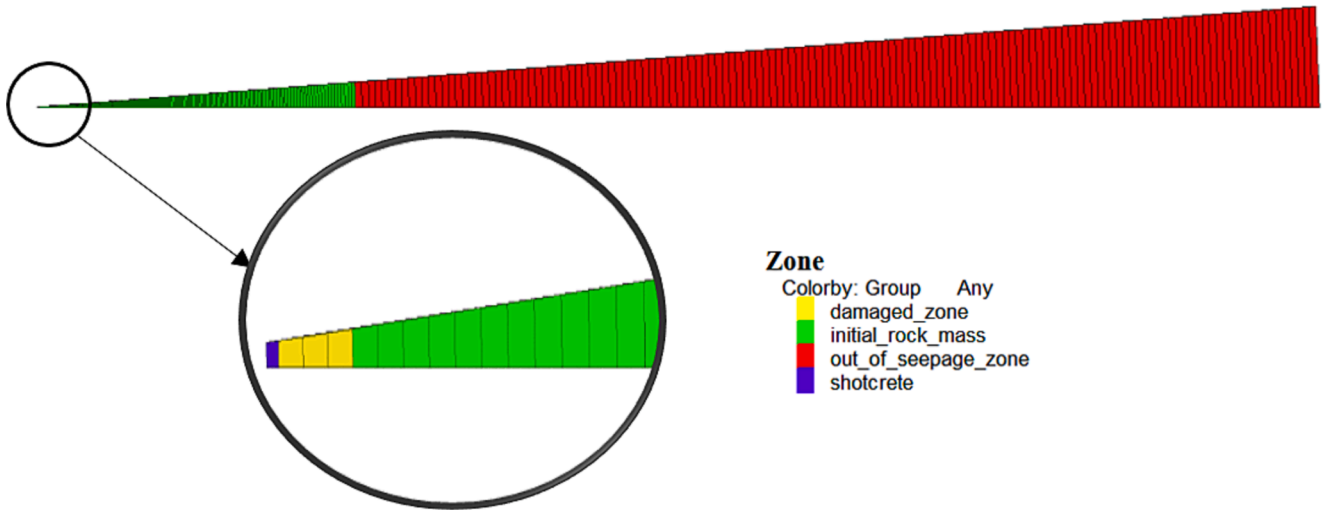

Fig. 3. The FLAC^{3D} model for the analysis of the creep behavior and groundwater flowing around a circular and deep tunnel.

Table 1
Mean, standard deviation values and variability intervals of the parameters treated probabilistically in the analyses.

Parameter	$\mu_{(*,**)}$	$\sigma_{(*)}$	$\mu-3\sigma$	$\mu+3\sigma$
GSI	30	1.67	25	35
σ_{ci}(MPa)	25	–	–	–
m_i	10	–	–	–
Kelvin shear modulus of rock mass ($G_{K(ini)}$) (MPa)	345	23	276	414
Maxwell viscosity of rock mass ($\eta_{M(ini)}$) (MPa. year)	132,500	–	–	–
Kelvin viscosity of rock mass ($\eta_{K(ini)}$) (MPa. year)	665	–	–	–
Kelvin shear modulus of damaged zone ($G_{K(alt)}$) (MPa)	$0.1G_{K(ini)}$	–	–	–
Maxwell viscosity of damaged zone ($\eta_{M(alt)}$) (MPa. year)	$0.1\eta_{M(ini)}$	–	–	–
Kelvin viscosity of damaged zone ($\eta_{K(alt)}$) (MPa. year)	$0.1\eta_{K(ini)}$	–	–	–
Rock mass permeability ($k_{(ini)}$) ($\frac{m}{s}$)	10^{-6}	6.66×10^{-8}	0.8×10^{-6}	1.2×10^{-6}
Lining elasticity modulus (GPa)	31.5	–	–	–
Lining Poisson's ratio	0.2	–	–	–
Damaged zone permeability ($k_{(ini)}$) ($\frac{m}{s}$)	$3k_{(ini)}$	–	–	–
Lining permeability ($\frac{m}{s}$)	10^{-7}	–	–	–
Damage zone thickness (t_{alt}) (m)	2	0.13	1.6	2.4
Lining thickness (m)	0.32	–	–	–
Initial water pressure in the rock mass along the tunnel wall axis (p_{w0}) (MPa)	2.72	–	–	–

* μ: mean value; σ: standard deviation.
** The mean values of parameters are selected based on the study of Do et al. [4] and Zaheri et al [35].

masses (both of damaged and undamaged zones) can be derived on the basis of equations proposed by Hoek et al. [16] in which the input data required are:

GSI (Geologic Strength Index of rock mass), σ_{ci} (uniaxial compressive strength of the intact rock), and m_i (Intact Rock strength parameter of Hoek and Brown strength criterion).

To stabilize the tunnel, a porous elastic lining is installed; it has a lower hydraulic conductivity than that one of the rock masses. On the other hand, after elapsing some time and after installation of the supporting system along its whole length (e.g., after 1 year), the tunnel will be filled with water to transfer it from a reservoir to the powerhouse.

Probabilistic Analysis

Numerical modeling of the problem

FLAC^{3D} software is used to simulate the behavior of pressurized tunnels. The behavior of the rock mass is elasto-viscoplastic governed by the CVISC model while the lining has an elastic behavior. The adopted steps of the numerical model are as follows:

- *Construction of the model geometry:* As the initial in-situ stress is hydrostatic and the axisymmetric symmetry is adopted, only a sector of the model is constructed (See Fig. 3). The size of the model along the tunnel axis is 1 m, in order to be able to simulate the plane-strain condition. Three different zones are considered:

i) EDZ, ii) a zone in which the water seepage occurs, and iii) a zone with a constant pore water pressure with the value that does not vary over time.

It is assumed that at distances greater than two times of the distance between the tunnel center and the groundwater surface, measured from the tunnel center, the water does not seep[19],

- *Applying the boundary conditions and initial stress state:* The initial total in-situ stress and pore water pressure are applied to all zones of the model. In addition, the same stress and pore water pressure are assigned to the tunnel boundary and to the right boundary shown in Fig. 3;
- *Assigning the constitutive model*: As stated, the CVISC model showing the elasto-viscoplastic behavior is assigned to the elements representing the rock mass, and the mechanical parameters of this model are assigned to them. Note that the values of the parameters attributed to the EDZ and to the rock mass are different. As the seepage of the water also takes place, it is necessary to apply a fluid-flow calculation for the water. For this purpose, the isotropic flow model is adopted; it uses a constant conductivity coefficient in the rock mass;
- *Solving the model*;
- *Initialization of the displacements and velocities to zero*;
- *Tunnel excavation:* the pore water pressure at the tunnel wall is set to zero;
- *Solving the model at time 0:* two different approaches can be conducted to simulate the hydro-mechanical interaction: coupled and

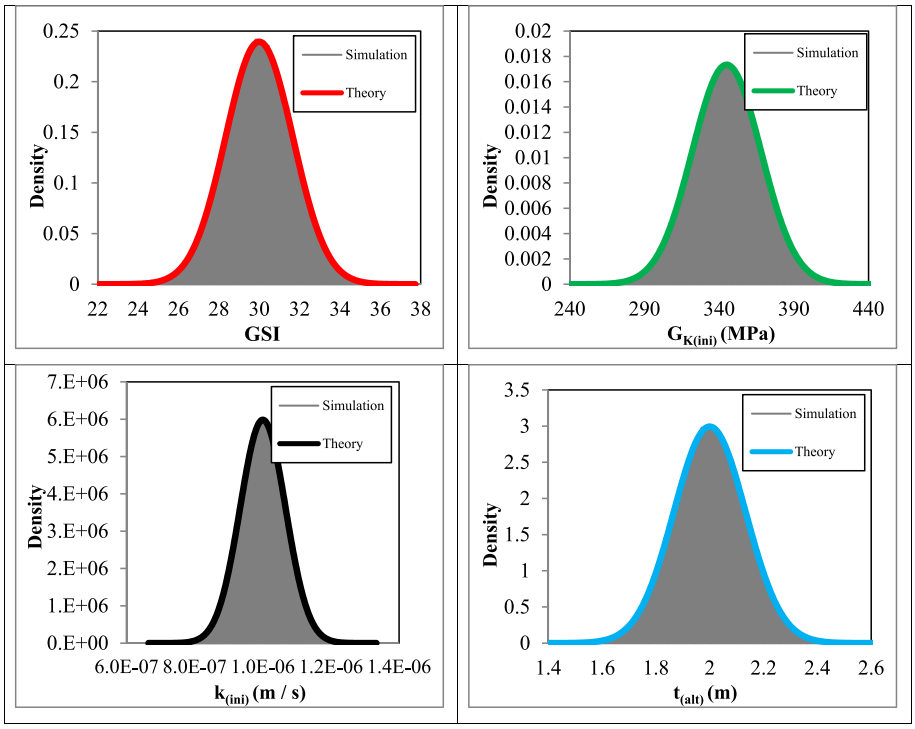

Fig. 4. Distribution functions (PDF) for the 4 probabilistic parameters considered in the analyses.

Table 2
The selected values of the input variables by response surface methodology and the calculated corresponding outputs using FLAC^{3D} software for Case 1.

	Random values of the selected parameters		Case 1	
Run	GSI	$G_{K(ini)}$ (MPa)	Displacement (m)	Lining pressure (MPa)
1	30	345	0.0741689	3.778416096
2	30	345	0.0741689	3.778416096
3	35	414	0.04320288	3.927225696
4	30	345	0.0741689	3.778416096
5	30	442.6	0.07342063	3.369154143
6	25	276	0.1393029	3.592029419
7	37	345	0.03610805	4.369568604
8	23	345	0.1846341	2.993312268
9	30	247.4	0.07512079	4.299047316
10	30	345	0.0741689	3.778416096
11	30	345	0.0741689	3.778416096
12	25	414	0.1381221	2.946163156
13	35	276	0.04435452	4.557109395

uncoupled. As the coupled hydro-mechanical analysis is time-consuming, the uncoupled analysis was performed and presented in this paper. Initially, the hydraulic analysis is performed and after obtaining the pore water distribution in the model, the mechanical analysis is conducted;

- *Performing the creep analyses till to lining installation*;
- *Setting the nodal velocities to zero*: when switching from the creep analysis to the static one, it is necessary to set the nodal velocities to zero before cycling because, if this step is not performed, the velocities will be inappropriate for the static analysis;
- *Lining installation:* In this step, an elastic lining is installed. Due to existing cracks in the lining, the water seeps through this medium. Thus, it is necessary to change the boundary conditions related to the pore pressure. It is assumed that at the outer radius of the lining the pore water pressure can vary with time, but at its inner radius, the pressure is fixed to zero;

Table 3
The selected values of the input variables by response surface methodology and the calculated corresponding outputs using FLAC^{3D} software for Case 2.

	Random values of the selected parameters			Case 2	
Run	GSI	$G_{K(ini)}$ (MPa)	$t_{(alt)}$ (m)	Displacement (m)	Lining pressure (MPa)
1	30	345	2	0.3958784	1.85845173
2	35	276	1.6	0.1928918	2.839065752
3	35	414	2.4	0.2932906	2.086266177
4	30	345	2	0.3958784	1.85845173
5	30	229	2	0.3966511	2.295647618
6	35	276	2.4	0.2941929	2.579745634
7	25	276	1.6	0.5495648	1.675653199
8	30	345	2.7	0.536041	1.735218609
9	30	345	1.3	0.2725149	2.08517223
10	25	276	2.4	0.8203972	1.494440892
11	25	414	2.4	0.8188218	1.164834684
12	30	461	2	0.3952933	1.554990854
13	38	345	2	0.1743527	2.815108314
14	30	345	2	0.3958784	1.85845173
15	30	345	2	0.3958784	1.85845173
16	35	414	1.6	0.1919266	2.311181664
17	25	414	1.6	0.5496692	1.305461561
18	22	345	2	1.005908	1.104886392
19	30	345	2	0.3958784	1.85845173
20	30	345	2	0.3958784	1.85845173

- *Solving the model and performing creep analyses till filling the tunnel with water*;
- *Setting the nodal velocities to zero*;
- *Filling the tunnel with water*: The tunnel is filled with water to transport water from a reservoir to a powerhouse. The pore water pressure and the total radial stress are set to the value of the internal water pressure on the inner radius of the lining;
- *Solving the model and performing creep analyses till the desired time.*

Table 4
The selected values of the input variables by response surface methodology and the calculated corresponding outputs using FLAC^{3D} software for *Cases 3 and 4*.

	Random values of the selected parameters			Case 3		Case 4	
Run	GSI	$G_{K(ini)}$(MPa)	$k_{(ini)}(\frac{m}{s})$	Displacement (m)	Lining pressure (MPa)	Displacement (m)	Lining pressure (MPa)
1	30	345	10^{-6}	0.07574	3.00598	0.06849	5.54192
2	35	276	8×10^{-7}	0.04232	3.57189	0.03450	5.80328
3	25	276	1.2×10^{-6}	0.15430	2.62527	0.14764	5.48504
4	35	414	8×10^{-7}	0.04188	3.33537	0.03413	5.60185
5	30	228.956	10^{-6}	0.07607	3.18628	0.06861	5.60702
6	22	345	10^{-6}	0.27515	2.18265	0.26950	5.59357
7	30	345	10^{-6}	0.07574	3.00598	0.06849	5.54192
8	25	414	8×10^{-7}	0.15390	2.40362	0.14795	5.65952
9	35	414	1.2×10^{-6}	0.04196	3.38089	0.03399	5.51601
10	25	276	8×10^{-7}	0.15420	2.56760	0.14795	5.65935
11	30	345	6.6×10^{-7}	0.07565	2.95847	0.06875	5.69353
12	30	345	1.3×10^{-6}	0.07582	3.05217	0.06823	5.40066
13	30	345	10^{-6}	0.07574	3.00598	0.06849	5.54192
14	30	345	10^{-6}	0.07574	3.00598	0.06849	5.54192
15	25	414	1.2×10^{-6}	0.15400	2.46320	0.14765	5.48619
16	30	461.044	10^{-6}	0.07545	2.84702	0.06848	5.54039
17	30	345	10^{-6}	0.07574	3.00598	0.06849	5.54192
18	30	345	10^{-6}	0.07574	3.00598	0.06849	5.54192
19	38	345	10^{-6}	0.03036	3.75233	0.02242	5.91580
20	35	276	1.2×10^{-6}	0.04239	3.61462	0.03456	5.82911

Table 5
The selected values of the input variables by response surface methodology and the calculated corresponding outputs using FLAC^{3D} software for *Cases 5 and 6*.

	Random values of the selected parameters			Case 5		Case 6	
Run	GSI	$G_{K(ini)}$(MPa)	$t_{(alt)}$(m)	Displacement (m)	Lining pressure (MPa)	Displacement (m)	Lining pressure (MPa)
1	30	345	2	0.30038	1.48650	0.29614	5.66728
2	35	276	1.6	0.13975	2.02108	0.13504	5.94220
3	35	414	2.4	0.20194	1.78316	0.19737	5.78892
4	30	345	2	0.30038	1.48650	0.29614	5.66728
5	30	229	2	0.30047	1.55712	0.29631	5.78405
6	35	276	2.4	0.20213	1.88993	0.19770	5.96668
7	25	276	1.6	0.46958	1.23700	0.46574	5.63906
8	30	345	2.7	0.39664	1.44611	0.39250	5.68371
9	30	345	1.3	0.21365	1.59602	0.20917	5.64626
10	25	276	2.4	0.67349	1.18531	0.66971	5.62318
11	25	414	2.4	0.67278	1.13324	0.66910	5.62362
12	30	461	2	0.30032	1.41748	0.29608	5.60273
13	38	345	2	0.12064	2.18521	0.11571	5.99223
14	30	345	2	0.30038	1.48650	0.29614	5.66728
15	30	345	2	0.30038	1.48650	0.29614	5.66728
16	35	414	1.6	0.13954	1.90053	0.13472	5.76552
17	25	414	1.6	0.46955	1.17672	0.46582	5.63901
18	22	345	2	0.95205	1.01255	0.94865	5.65262
19	30	345	2	0.30038	1.48650	0.29614	5.66728
20	30	345	2	0.30038	1.48650	0.29614	5.66728

Generation of random values for probabilistic variables

Rock mass properties can vary from one point to another point, and thus, it is reasonable to use a range of values for a parameter (probabilistic approach) instead of using a single one (i.e., the mean value, deterministic approach). According to Hoek [14], the normal distribution can best explain the uncertainty of rock mass properties; it can be described by the mean and the standard deviation of each parameter.

In the case of tunnels excavated in rock masses with time-dependent behavior, the followings are the influential parameters:

- those controlling the strength of the rock mass (Hoek and Brown strength criterion), including: σ_{ci}, GSI, and m_i;
- those controlling the long-term response of the tunnel, including: Kelvin viscosity ($\eta_{K(ini)}$), Maxwell viscosity ($\eta_{M(ini)}$), and Kelvin shear modulus ($G_{K(ini)}$); and
- Rock mass permeability ($k_{(ini)}$) and the *EDZ* thickness ($t_{(alt)}$).

Three random parameters are selected for analyses of each case (see section entitled "Results and discussions"): one among σ_{ci}, GSI, and m_i (which controls the short-term behavior), another one among $\eta_{K(ini)}$, $\eta_{M(ini)}$, and $G_{K(ini)}$ (which controls the long-term behavior); and finally one from $k_{(ini)}$ and $t_{(alt)}$(which controls the seepage force or the excavation quality). Based on the parametric study (available in Appendix B), the parameters GSI, $t_{(alt)}$, and $G_{K(ini)}$ are selected for those cases that have the EDZ around the tunnel profile. However, $t_{(alt)}$ is replaced by $k_{(ini)}$ for those that do not have an EDZ around the tunnel profile.

To generate random values, it is necessary to assume a mean value and a standard deviation value for each selected variable adopting a normal probabilistic distribution. For example, the standard value of GSI was selected as 1.67, since 99.73 % of GSI values will be in the range of $GSI^{mean} \pm 3\times1.67 = GSI^{mean} \pm 5$. That is, the range of generated values will be in GSI^{mean} −5 to GSI^{mean} +5 interval (for 99.73 % of cases), as the suggested range of GSI by Hoek and Marinos [15]. For the other parameters, the standard deviation σ is assumed in such a way as to have a

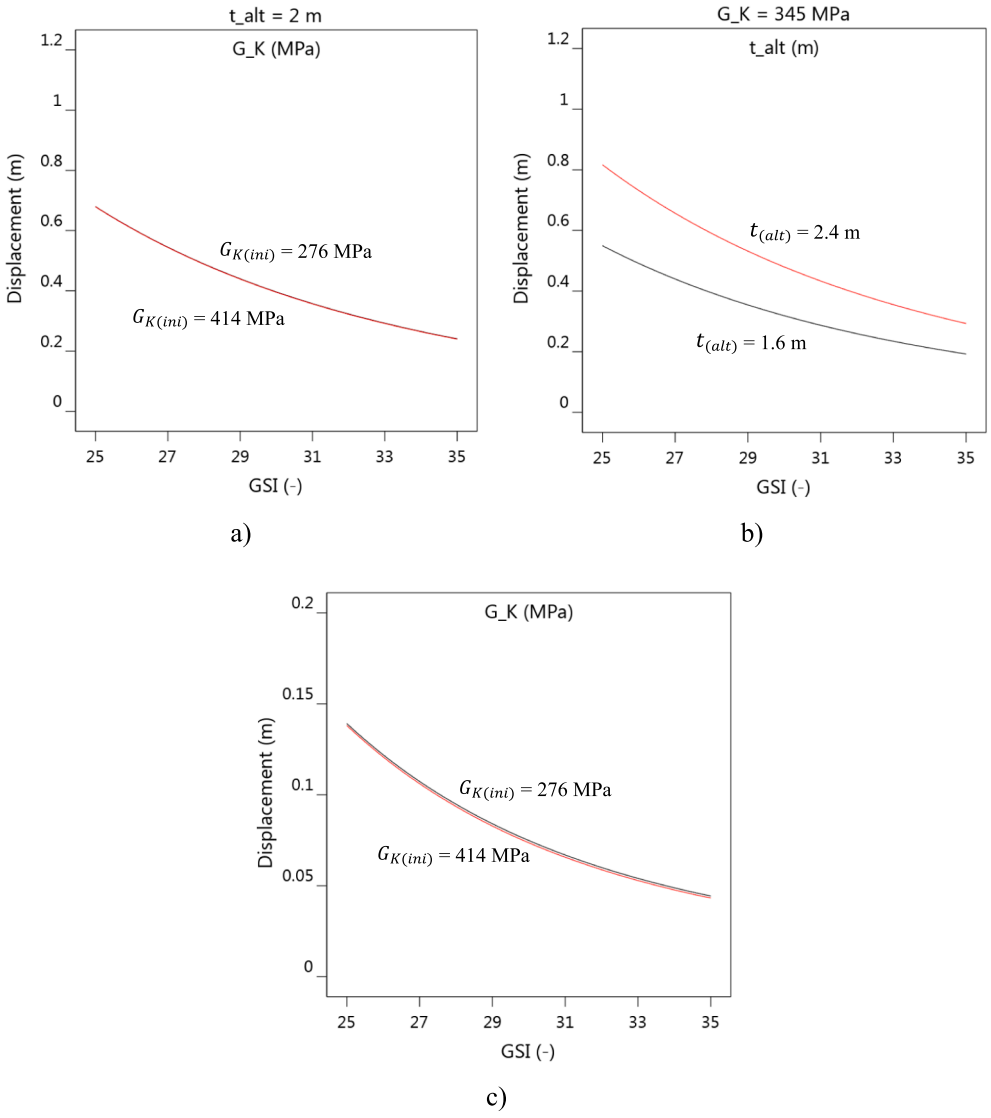

Fig. 5. Tunnel wall displacement at t = 5-year a) Case 2 (constant $t_{(alt)}$), b) Case 2 (constant $G_{K(ini)}$), c) Case 1.

value so that the range $\pm 3\sigma$ covers the whole range of $\pm$ 20 % of the mean value. That is, 3σ= 20 % of the mean value (Table 1).

Fig. 4 shows the distributions (normal distributions) of the probabilistic parameters assumed in the analyses (Table 1).

The Monte Carlo method is then used to generate random values starting from the probabilistic distribution functions.

Response surface methodology (RSM) to select only some results by the Monte Carlo Method (MCM)

As the Monte Carlo Method generates many random values for each selected variable, the response surface methodology is here used to select only few of them[23]. The Response Surface Methodology (RSM) is a set of statistical techniques and applied mathematics that determines the relationship between output and independent input variables. It uses an iterative process to create models among variables. As the model is determined, it is examined to check its satisfaction. The aim is to explore a suitable fitting function between the output of the problem and inputs with the least number of tests.

For this purpose, the minimum and the maximum values of each random parameter are imported into *Design-expert* software to generate the function. The general equation of the response surface for the quadratic state is

$$G(x) = a_0 + \sum_{i=1}^{n} a_i x_i + \sum_{i=1}^{n} \sum_{j=1}^{n} b_{ij} x_i x_j \quad (1)$$

where a_i and b_{ij} are the coefficients calculated by the software, and x_i and x_j are random variables. The first and second terms show the main effects of the variables whereas the third one illustrates the effects of the non-linearity of the variables. Besides, n is the number of the random parameters.

Finally, the software intelligently selects appropriate sets of parameter values so that they almost cover all of the required analyses. Tables 2- 5 give the detailed result of RSM analyses for the intelligent selection of values of variables for *Cases 1–6* to be used as input in FLAC^{3D}.

Results and discussions

The response of a tunnel in the following six cases was investigated by the developed numerical model:

- Case 1: dry rock mass after elapsing 5 years;
- Case 2: same condition as Case 1 but with an EDZ around the tunnel;

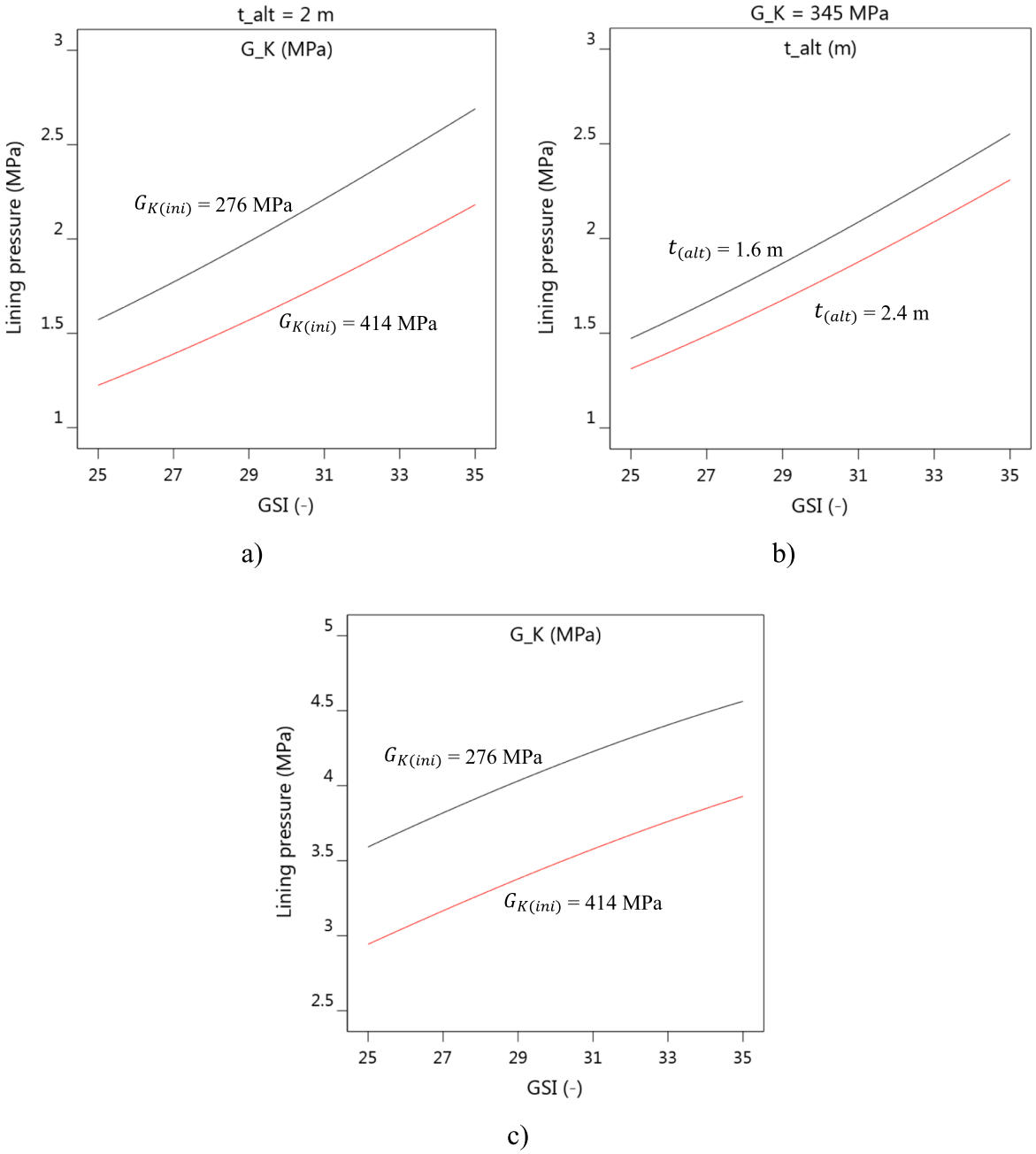

Fig. 6. Lining pressure at t = 5-year a) Case 2 (constant $t_{(alt)}$), b) Case 2 (constant $G_{K(ini)}$), c) Case 1.

- Case 3: in a saturated uniform rock mass before applying the internal water pressure to the tunnel (i.e., 1 year);

- Case 4: same condition as Case 3 but after applying the internal water pressure (i.e., 5 years);

- Case 5: same condition as Case 3 but with an EDZ around the tunnel; and

- Case 6: same condition as Case 4 but with an EDZ around the tunnel.

In Appendix A, the verification of the accuracy of the simulation using the numerical modeling is presented: the results of the numerical calculation are compared with the ones of the analytical method proposed by Zaheri et al. [35]. For this purpose, the mean values of the parameters of Table 1 are used without considering the excavation damaged zone, since the analytical method is not able to take it into account.

Effectiveness of variables by response surface methodology (RSM)

If the data sets of random variables for each *Case* (available in Tables 2-5) together with corresponding outputs by FLAC^{3D} are introduced to the RSM, it is possible to derive the relationship between each output variable and all input parameters. Hence, the weight and role of any variable in each output is explored for the considered *Cases*. Figs. 5-8 illustrate the effect of considered random variables on the tunnel convergence and tunnel lining pressure, varying the random variables, obtained by the RSM.

For the *Cases* of tunneling in the dry rock mass (i.e., *Cases 1 and 2*), as expected, increasing GSI and $G_{K(ini)}$ causes the tunnel wall displacement to decrease. However, their effects on the lining pressure are different.

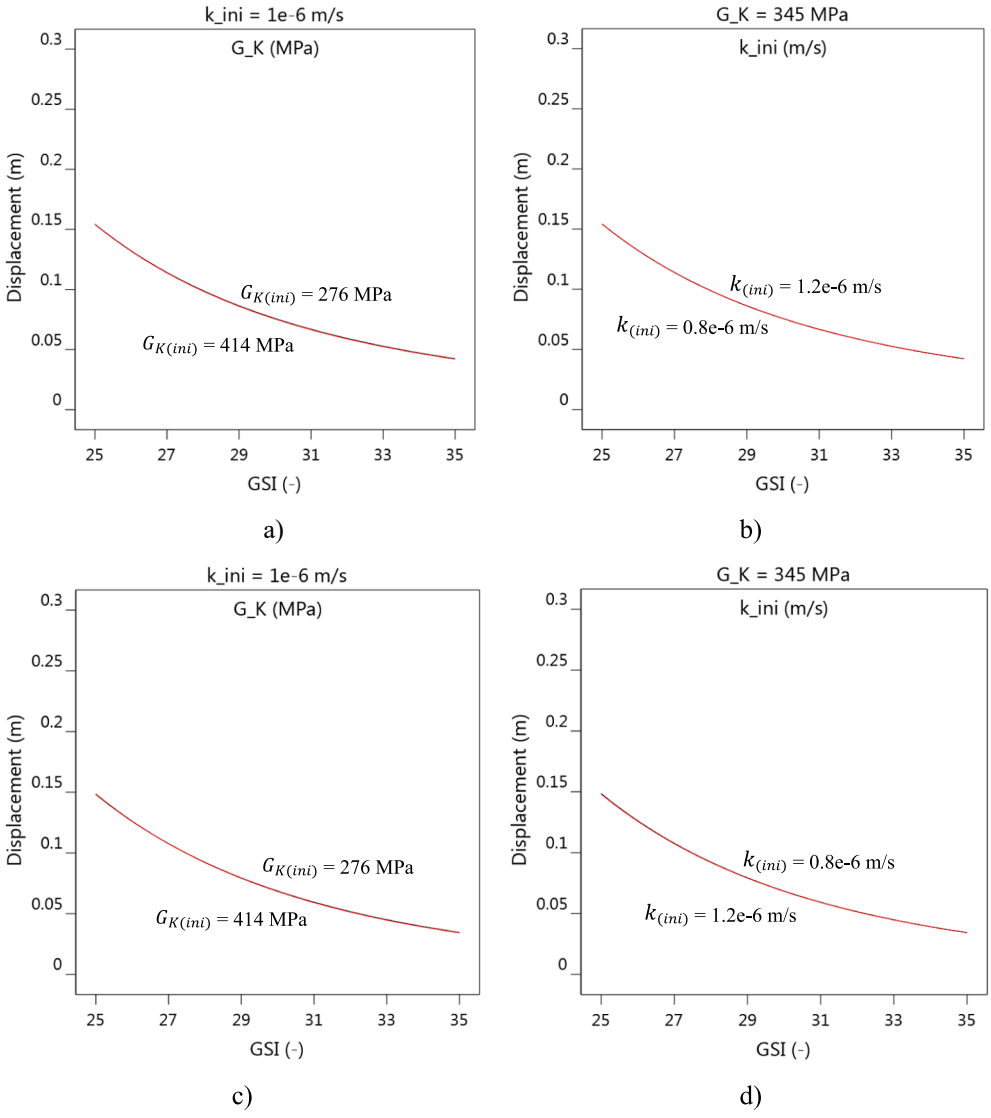

Fig. 7. Tunnel wall displacement a) Case 3 (constant $k_{(ini)}$), b) Case 3 (constant $G_{K(ini)}$), c) Case 4 (constant $k_{(ini)}$), d) Case 4 (constant $G_{K(ini)}$), e) Case 5 (constant $t_{(alt)}$), f) Case 5 (constant $G_{K(ini)}$), g) Case 6 (constant $t_{(alt)}$), h) Case 6 (constant $G_{K(ini)}$).

That is, the lining pressure enhances with increasing GSI value, but the reverse condition occurs by increasing the $G_{K(ini)}$ parameter.

When a tunnel is embedded in a saturated medium, before applying the internal water pressure and at time = 1 year, the damaged zone thickness ($t_{(alt)}$) greatly influences both lining pressure and tunnel wall displacement. For instance, when $G_{K(ini)}$ = 345 MPa, if the $t_{(alt)}$ parameter becomes 1.5 times greater, the tunnel wall displacement becomes 42 % greater. For the case in which the EDZ does not exist (Case 3), increasing the rock mass permeability coefficient leads both the tunnel wall displacement and the lining pressure to increase. This is because enhancing the permeability leads the value of the pore water pressure behind the lining to increase. It also leads the plastic strains to increase; however, the effects of both $G_{K(ini)}$ and $k_{(ini)}$ are negligible with respect to the GSI which controls both the deformational modulus and the shear strength of the rock mass. When $G_{K(ini)}$ = 345 MPa, increasing the $k_{(ini)}$ value by 50 % causes the lining pressure to increase of 6.3 % and 2.6 %, for GSI = 25 and 35, respectively. On the other hand, for $k_{(ini)} = 10^{-8\frac{m}{s}}$, if the $G_{K(ini)}$ parameter becomes 1.5 times greater, the pressure exerting on the lining decreases of 6.7 % and 6.3 %, for GSI = 25 and 35, respectively.

All of the above-stated comments about the tunnel displacements, except the influence of the rock mass permeability, can be extended to the case in which the internal water pressure is applied on the lining (*Cases 4 and 6*). Indeed, as the water seeps outward (i.e., from the tunnel toward the rock mass), the rock mass displacements greatly decrease.

Reliability results - Probability density functions for the tunnel convergence and pressure exerted on the lining

By substituting the relationship obtained from the RSM in the code (MATLAB software) defined for the Monte Carlo method, the probability density functions of outputs are obtained. In Fig. 9, the PDFs of outputs are depicted for *Cases 3 and 4*. As observed, the *Gamma* distribution is the best-fit probability density function for outputs of these studied cases (the same applies to the other studied cases), although the input values obey the *Normal* distribution. The mean, standard deviation, Mode, and Skewness of the obtained *Gamma* distribution for all the studied cases are summarized in Table 6.

Reminding the *Mode* is the value that occurs most frequently in a data set (i.e., the point at which the probability density function reaches its maximum value). *Skewness* represents the asymmetry of a

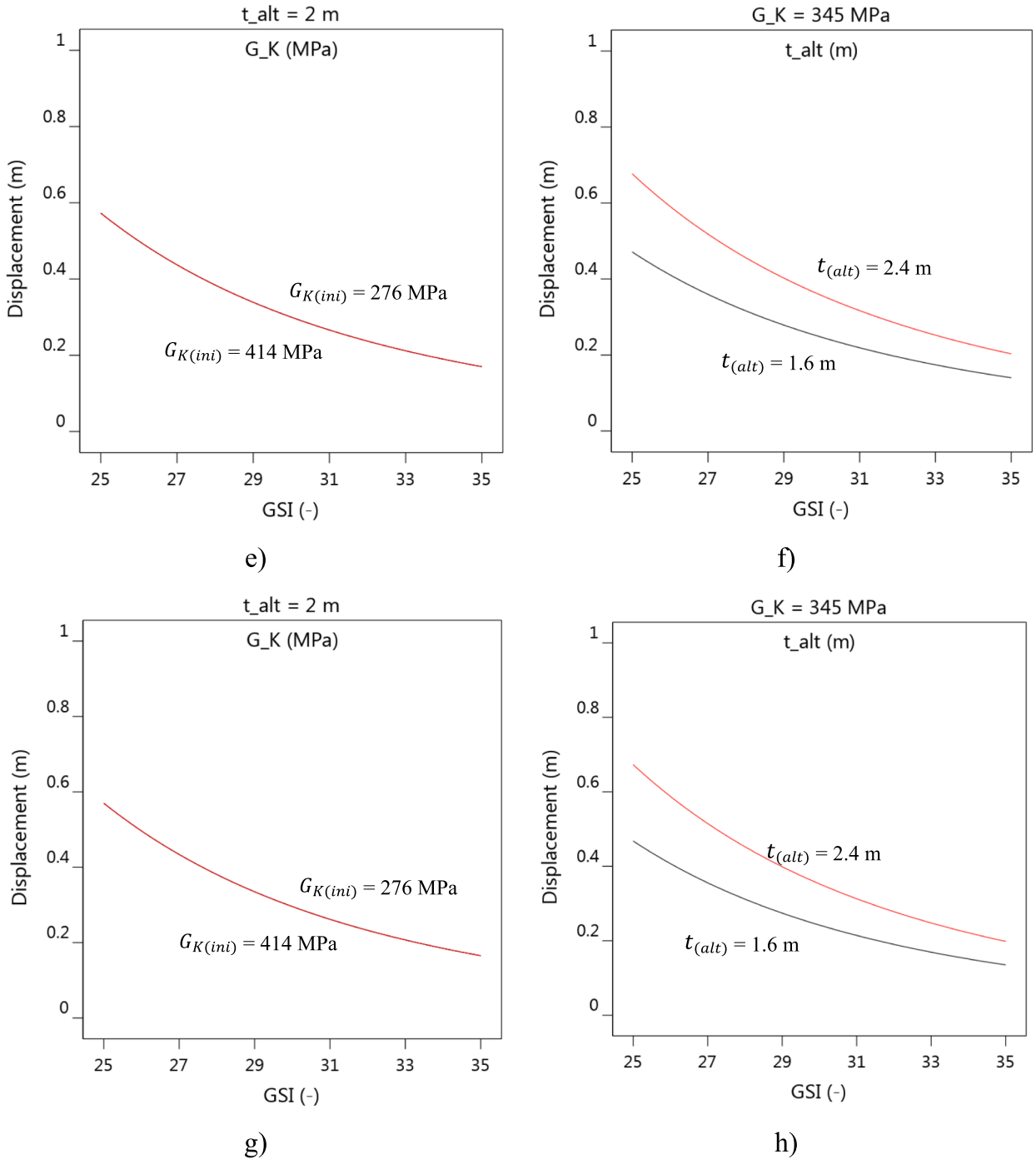

Fig. 7. (*continued*).

distribution around its mean value.

As noticed in Table 6, it can be concluded that in all 6 cases, the *mean* value is greater than the *mode,* for both the tunnel wall displacement and the lining stress. Due to the specific characteristics of the *Gamma* distribution, the output distributions are right-skewed, meaning that the tails of the distribution curves are longer on the right side. It implies that the likelihood of the output (tunnel displacement or lining stress) being less than its *mean* value is higher than 50 %. As an example, for Case 4, the *mean* value of the tunnel displacement is 7 cm, while the most probable value (*mode*) of the displacement is 6.6 cm. About displacements, the reason for such condition can be due to the GSI effect which impresses both the deformation modulus and shear strength of the EDZ and rock mass. The more the deformation modulus of the rock mass and the EDZ, the lower the tunnel convergence. On the other hand, the greater $t_{(alt)}$ is, the greater tunnel convergence is. But as can be seen in Figs. 5-8, the GSI effect is more dominant than the excavation damaged zone thickness.

Compared to the cases in which the internal water pressure is not applied, the skewness of the displacement distribution increases for the condition after the internal pressure is applied. But on the other hand, a reverse condition occurs with the lining pressure. In addition, when tunneling in a saturated rock mass, the skewness of displacement distribution is greater than that of the case in which the seepage flow is disregarded. Finally, the skewness of the lining pressure distribution is much smaller than that of the displacement distribution. Thus, it can be

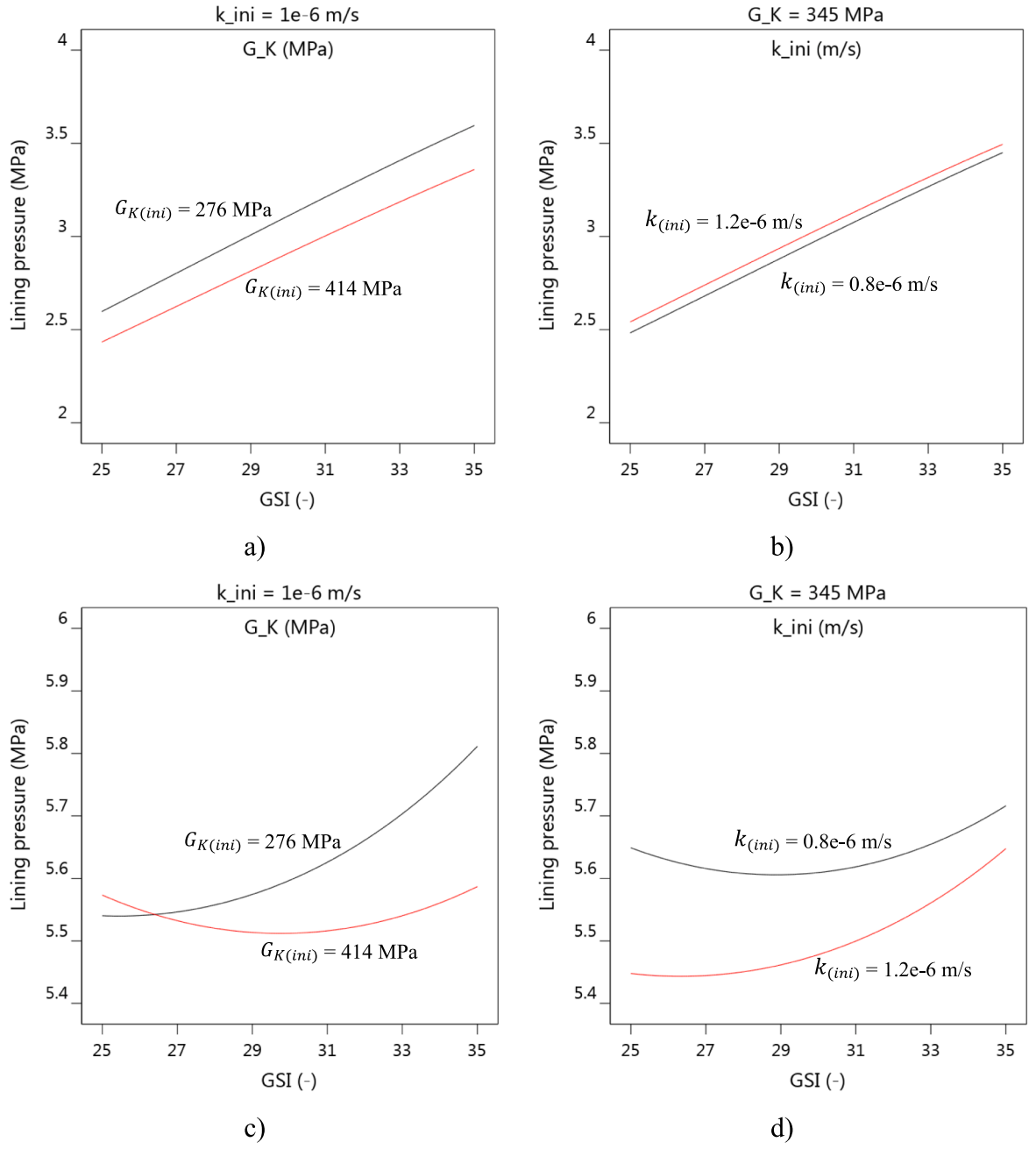

Fig. 8. Lining pressure a) Case 3 (constant $k_{(ini)}$), b) Case 3 (constant $G_{K(ini)}$), c) Case 4 (constant $k_{(ini)}$), d) Case 4 (constant $G_{K(ini)}$), e) Case 5 (constant $t_{(alt)}$), f) Case 5 (constant $G_{K(ini)}$), g) Case 6 (constant $t_{(alt)}$), h) Case 6 (constant $G_{K(ini)}$).

said that the PDF of lining pressure is almost symmetric around its mean. Therefore, in such a condition, the difference between the most probable and *mean* lining stress is small; and thus, there is a higher confidence in the results of the deterministic analysis.

In Fig. 10, the cumulative distribution function (CDF) of radial displacements of the tunnel wall for Case 4 is illustrated. This function represents the probability of a random parameter (here the tunnel displacement, but it can be also the lining pressure) to be less than or equal to a certain specific value. For instance, for Case 4, the probability of the tunnel displacement to be smaller than or equal to 6 cm is about 30 %.

Comparison of results of the deterministic and probabilistic analyses

The tunnel wall displacement and the lining stress values obtained by the deterministic and probabilistic analyses are summarized in Table 7. As can be seen, the difference of results in these approaches in predicting the lining stress is negligible. On the other hand, about 6 % of difference exists in the prediction of the tunnel wall displacement for the two different approaches. Moreover, the most probable value of the displacement (*mode*) in the probabilistic method is lower than the mean in the deterministic analysis. Besides, this percentage difference is higher when the water seepage is taken into account.

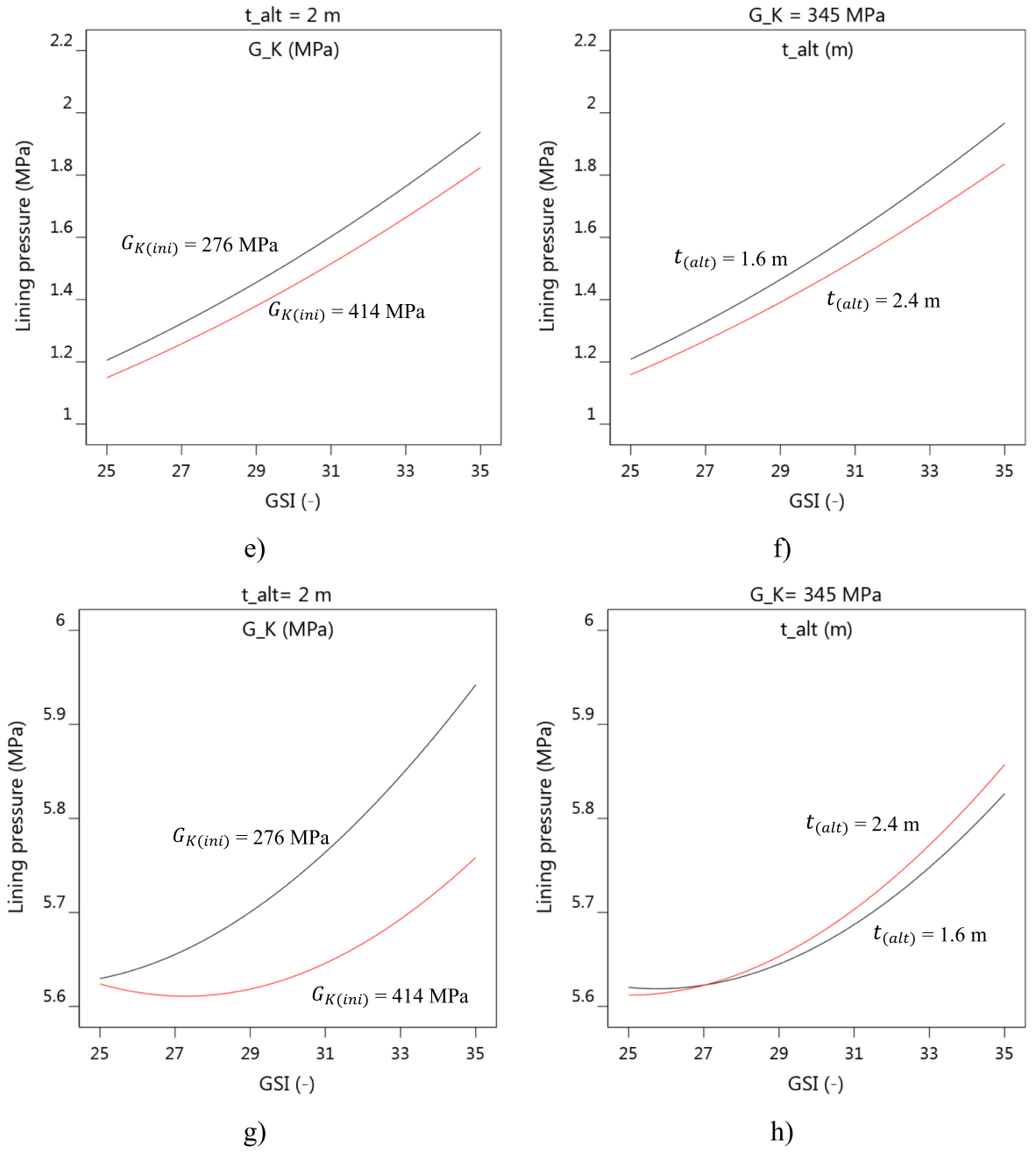

Fig. 8. (*continued*).

Conclusions

In this paper, probabilistic analyses were developed to take into account the uncertainty of rock mass parameters in designing underwater lined tunnels embedded in a rock mass with a rheological behavior. The presence of the excavation damaged zone due to poor blasting was also considered. Analyses were conducted using a finite difference code (FLAC^{3D} software).

Four parameters including the Geological Strength Index (GSI), rock mass permeability, thickness of the damaged zone, and Kelvin shear modulus were selected as probabilistic parameters. The response surface methodology was used to intelligently select the values of parameters from the sample obtained by the Monte Carlo method. After obtaining outputs by FLAC^{3D} in terms of datasets, the relationships between the input and output parameters were obtained by using the RSM. Then, the probability distribution functions of the main obtained results (tunnel wall displacement and lining pressure) were calculated. The results show that:

- The outputs can be represented by right-skewed Gamma distributions, (i.e., the distribution mass is concentrated on the left side of the probability distribution); It means that the design of these tunnels by deterministic analysis (which is done by mean value of variables) is not the most probable scenario which can occur in practice.
- The right-skewed Gamma distributions indicates that deterministic analysis result in a little unsafe design. The more right-skewness, the more instability potential, and the less expected safety factor from the design by deterministic analysis.
- GSI is the most effective parameter on the skewness of the probability distribution (compared to rheological properties of rock mass and permeability of rock mass), particularly in lower values. Hence,

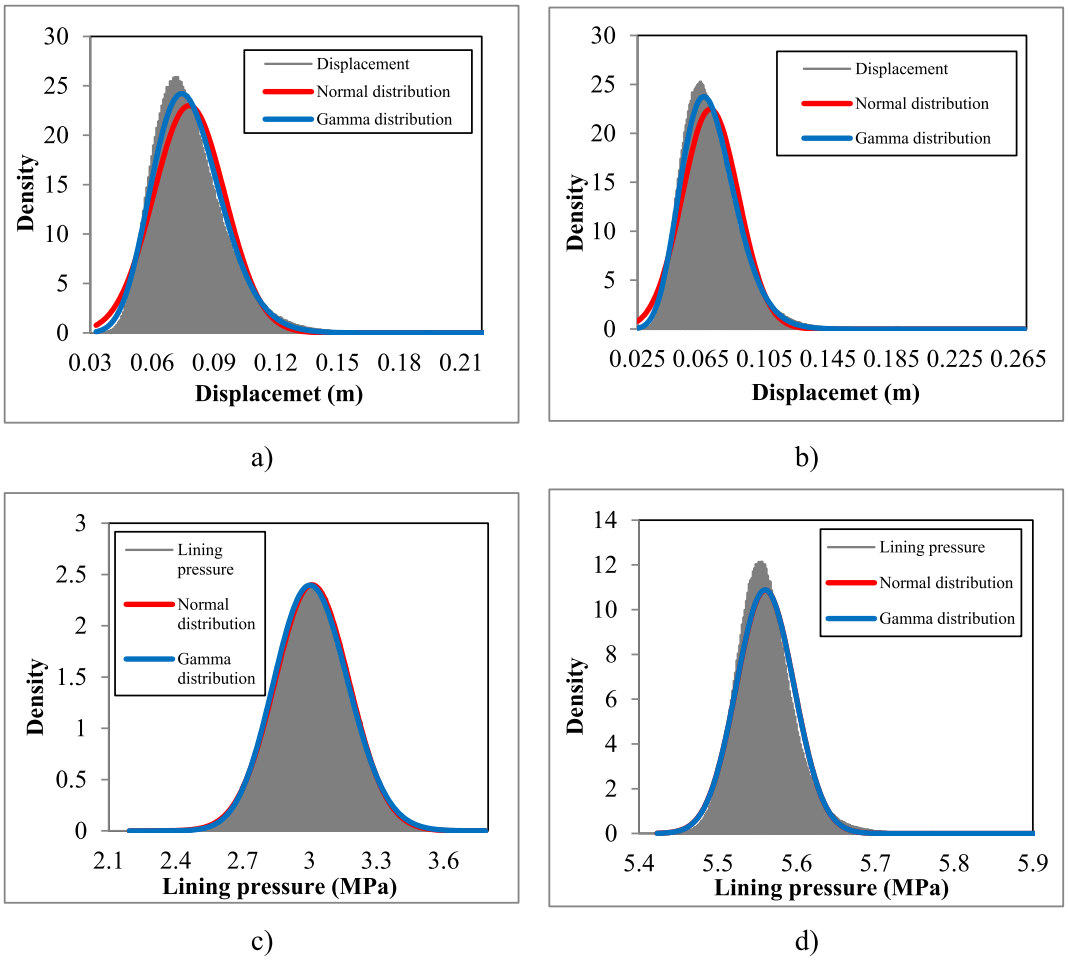

Fig. 9. Probability density functions of a) tunnel wall displacement (Case 3), b) tunnel wall displacement (Case 4), c) lining pressure (Case 3), d) lining pressure (Case 4).

Table 6
The characteristics of the *Gamma* probability distribution for the tunnel displacement and lining stress in all the studied cases.

		Mean	Standard deviation	Mode	Skewness
Case 1	Tunnel wall displacement	0.07664 (m)	0.01469 (m)	0.07382 (m)	0.38335
	Lining stress	3.75362 (MPa)	0.19653 (MPa)	3.74333 (MPa)	0.10471
Case 2	Tunnel wall displacement	0.40262 (m)	0.07481 (m)	0.38873 (m)	0.37159
	Lining stress	1.86682 (MPa)	0.19059 (MPa)	1.84736 (MPa)	0.20419
Case 3	Tunnel wall displacement	0.07796 (m)	0.01681 (m)	0.07434 (m)	0.43116
	Lining stress	3.01092 (MPa)	0.16672 (MPa)	3.00170 (MPa)	0.11074
Case 4	Tunnel wall displacement	0.07092 (m)	0.01723 (m)	0.06673 (m)	0.48581
	Lining stress	5.56026 (MPa)	0.03665 (MPa)	5.56003 (MPa)	0.01318
Case 5	Tunnel wall displacement	0.30812 (m)	0.06492 (m)	0.29444 (m)	0.42143
	Lining stress	1.49285 (MPa)	0.11935 (MPa)	1.48330 (MPa)	0.15990
Case 6	Tunnel wall displacement	0.30407 (m)	0.06532 (m)	0.29003 (m)	0.42963
	Lining stress	5.67514 (MPa)	0.04293 (MPa)	5.67480 (MPa)	0.01513

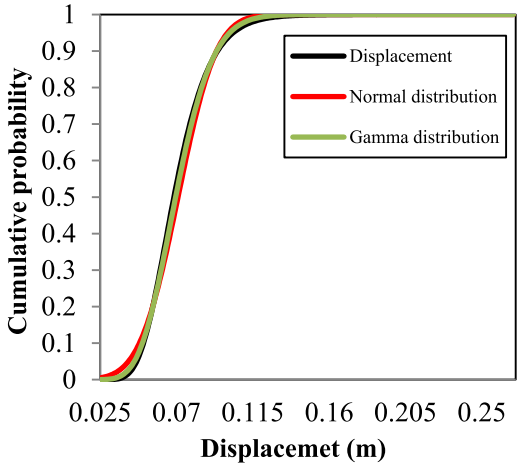

Fig. 10. The cumulative distribution function of tunnel wall displacement for Case 4.

referring to the above conclusion, more care is required in important projects when GSI is low.

- The skewness of the probability distribution function of displacements increases after applying the internal water pressure. But on the other hand, a reverse condition occurs with the lining pressure.

Table 7
The values of the tunnel wall displacements and lining pressure using the deterministic and probabilistic approaches.

	Mean value in the deterministic analysis		Most probable value (Mode) of the probability density function in the probabilistic analysis		Difference of predictions in the deterministic and probabilistic analyses (%)	
Case	Displacement (m)	Lining pressure (MPa)	Displacement (m)	Lining pressure (MPa)	Displacement	Lining pressure
1	0.07417	3.77842	0.07079	3.77213	4.77	0.17
2	0.39588	1.85845	0.37986	1.85721	4.22	0.07
3	0.07574	3.00598	0.07182	2.99275	5.46	0.44
4	0.06849	5.54192	0.06420	5.55497	6.69	−0.23
5	0.30038	1.48650	0.28095	1.48766	6.91	−0.08
6	0.29614	5.66728	0.27911	5.65096	6.10	0.29

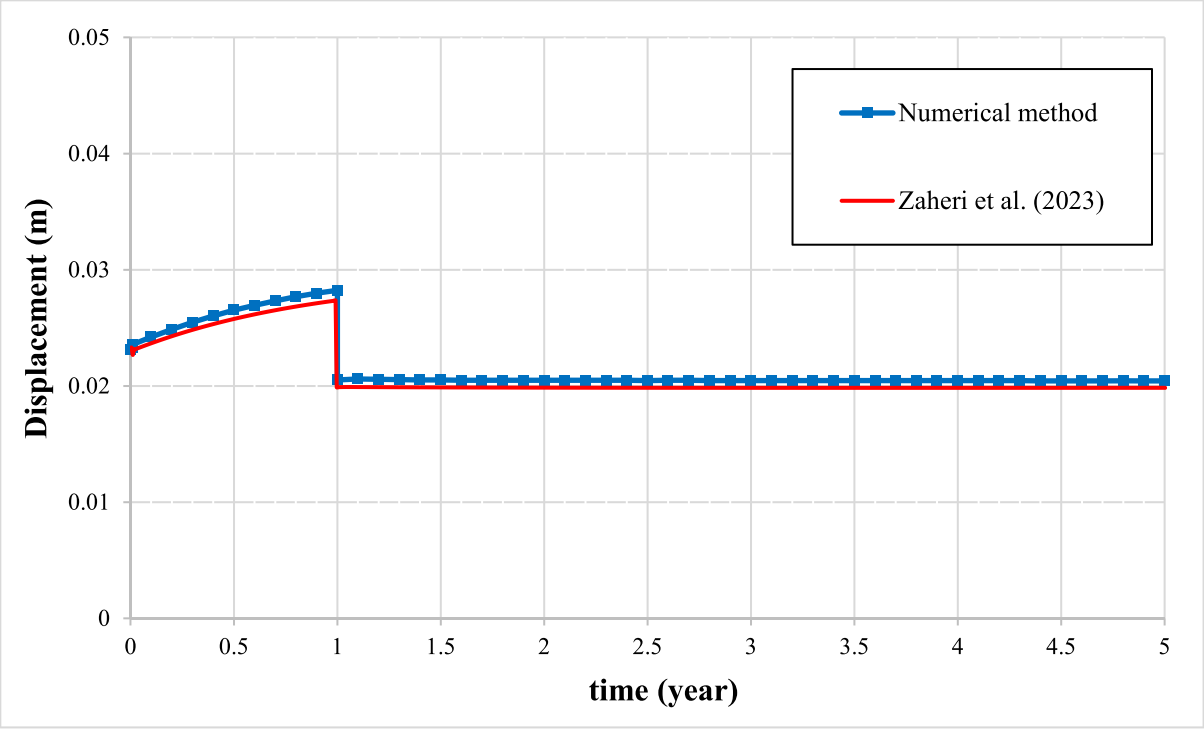

Fig. A1. Comparison between the results of the analytical and numerical methods.

- As time passes, depending on rheological parameter values and the extent of EDZ, the difference of design by probabilistic and deterministic analyses becomes greater.

Funding and Competing interests

The authors have no competing interests to declare that are relevant to the content of this article. Also, the authors did not receive support from any organization for the submitted work.

CRediT authorship contribution statement

Milad Zaheri: Data curation, Formal analysis, Software, Visualization, Writing – original draft. **Masoud Ranjbarnia:** Conceptualization, Data curation, Formal analysis, Investigation, Methodology, Resources, Software, Supervision, Validation, Writing – original draft, Writing – review & editing. **Pierpaolo Oreste.:** Investigation, Methodology, Supervision, Validation, Visualization, Writing – review & editing.

Declaration of competing interest

The authors declare that they have no known competing financial interests or personal relationships that could have appeared to influence the work reported in this paper.

Data availability

No data was used for the research described in the article.

Appendix A

Verification of the numerical simulation with FLAC^{3D}

To verify the accuracy of the simulation, the results of the numerical model are compared with the results of the analytical method proposed by Zaheri et al.[35]. For this purpose, the mean values of the parameters presented in Table 1 are used (the excavation damaged zone is not considered in the above-mentioned analytical method).

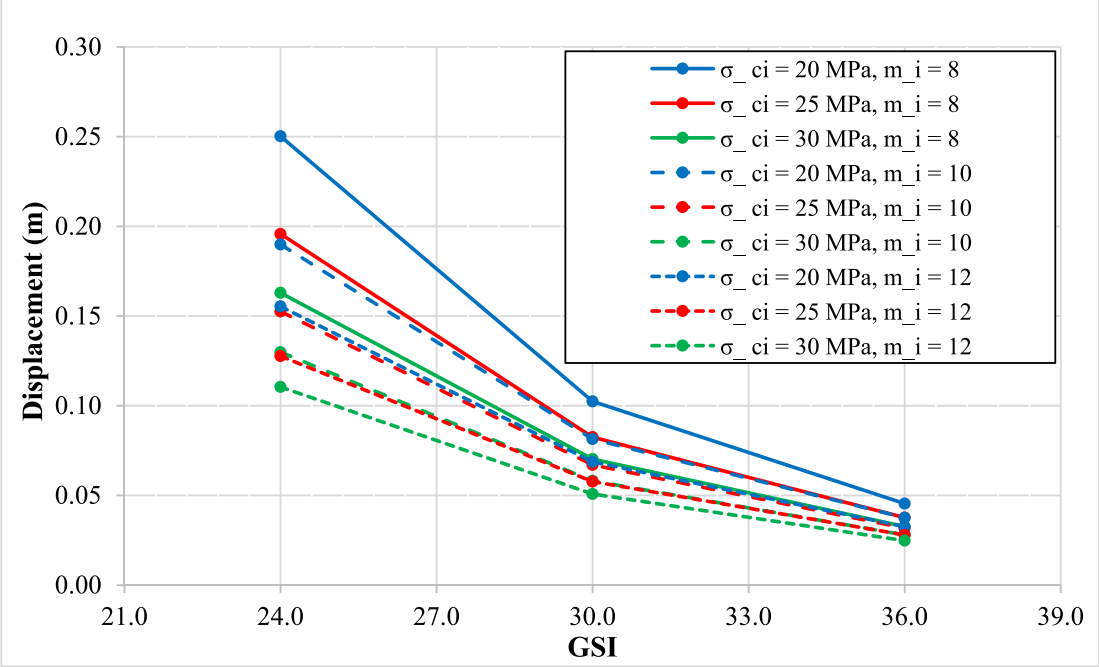

Fig. B1. Effect of parameters on the short-term displacements of the tunnel (dry condition).

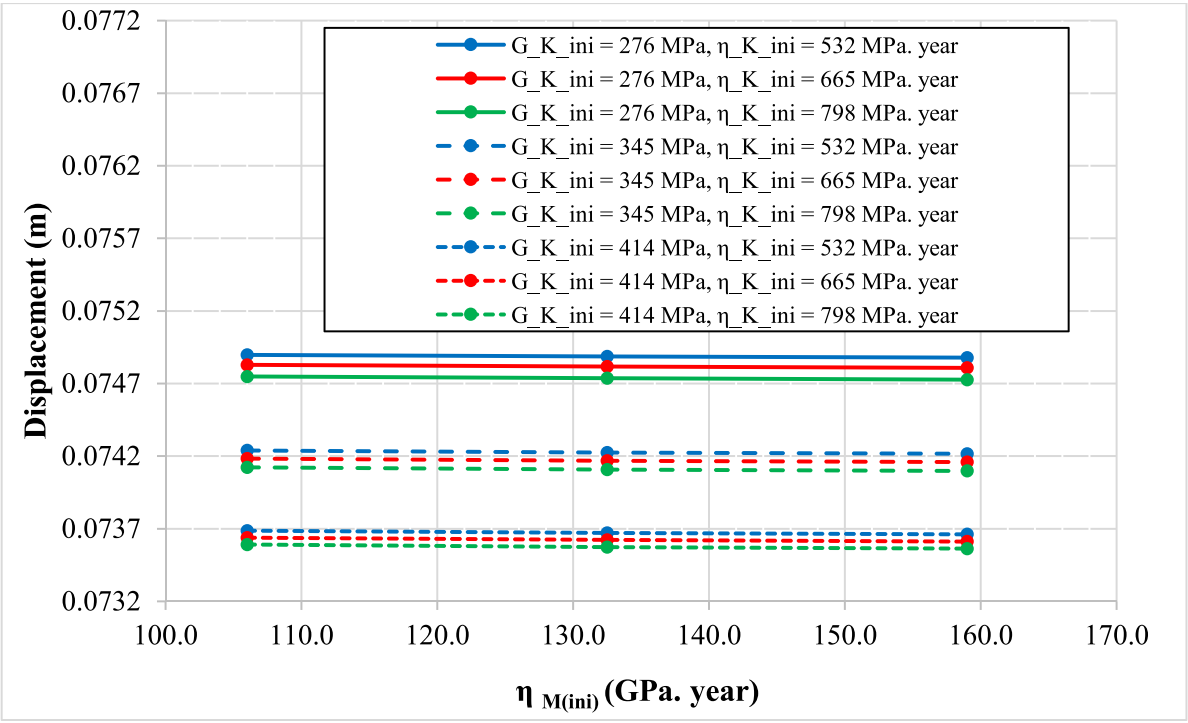

Fig. B2. Effect of different parameters on the long-term displacements of the tunnel wall at $t = 5$ years (dry condition).

It is assumed that the tunnel radius is 4.5 m and is excavated at a depth of 272 m from the surface. The tunnel lining is installed after 4 days, and the tunnel is filled with water after 1 year; the internal water pressure is equal to $2.4p_{w0}$.

Fig. A.1 presents the tunnel wall displacements over time for the two methods. As observed, there is a good agreement between the obtained results.

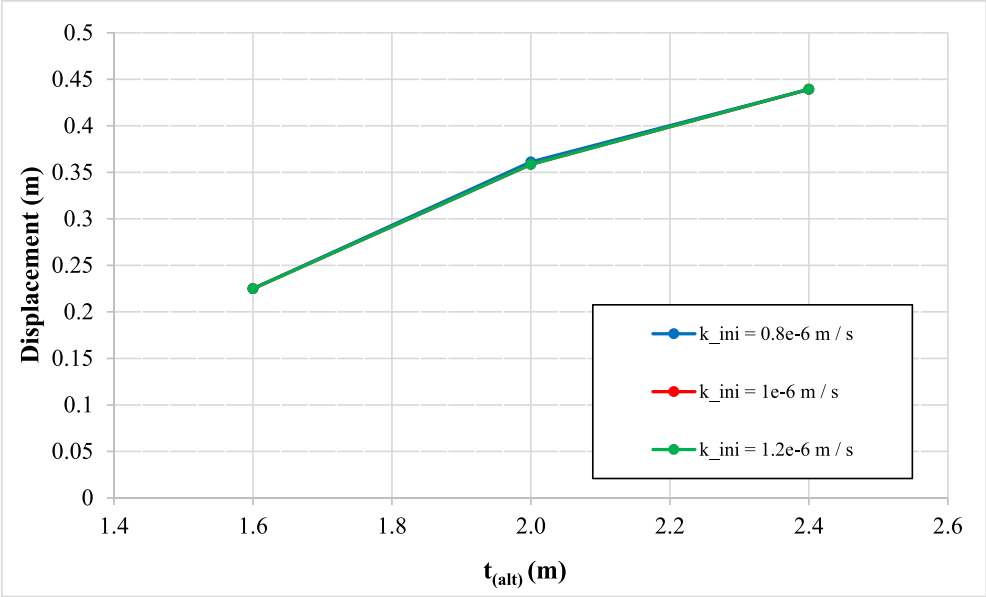

Fig. B3. Effect of rock mass permeability and of damaged zone thickness on the long-term displacements of the tunnel wall at $t = 5$ years (saturated condition).

Appendix B

Parametric study

Sensitive analyses are carried out to find the most influencing parameters, since it might be sufficient to consider them with a probabilistic approach and all the others with a deterministic one. The influences of the σ_{ci}, GSI, and m_i parameters on the instantaneous displacement of the tunnel excavated in a dry rock mass are investigated (Fig. B.1) (the existence of the EDZ is disregarded). As observed, GSI is the most important parameter, which greatly influences both the deformational modulus and the rock mass strength.

Similarly, among the parameters controlling the long-term response of the tunnel (i.e., $\eta_{K(ini)}$, $\eta_{M(ini)}$, and $G_{K(ini)}$), as seen in Fig. B.2, the Kelvin shear modulus of the rock mass has the greatest influence on the tunnel response at the time $t = 5$ years.

Finally, between the rock mass permeability and the EDZ thickness, as shown in Fig. B.3, the rock mass permeability shows a negligible influence, and thus, the thickness of the excavation damaged zone is selected for further probabilistic analysis.

For the cases in which an EDZ develops around the tunnel, three parameters including GSI, excavation damaged zone thickness, and Kelvin shear modulus are selected for the probabilistic approach. However, when the EDZ does not develop around the tunnel, the rock mass permeability is used instead of the EDZ thickness in this type of analysis.

References

[1] Brown, E., Bray, J. Rock-support interaction calculations for pressure shafts and tunnels. 1982 Paper presented at the ISRM International Symposium.

[2] Chu Z, Wu Z, Liu Q, Liu B. Analytical Solutions for Deep-Buried Lined Tunnels Considering Longitudinal Discontinuous Excavation in Rheological Rock Mass. J Eng Mech 2020;146(6):04020047. https://doi.org/10.1061/(ASCE)EM.1943-7889.0001784.

[3] Chu Z, Wu Z, Liu Q, Liu B, Sun J. Analytical Solution for Lined Circular Tunnels in Deep Viscoelastic Burgers Rock Considering the Longitudinal Discontinuous Excavation and Sequential Installation of Liners. J Eng Mech 2021;147(4): 04021009. https://doi.org/10.1061/(ASCE)EM.1943-7889.0001912.

[4] Do DP, Guo X, Dias D. Probabilistic Stability Analysis of Deep Rock Tunnel Excavated by Mechanized Tunneling Considering Anisotropic Initial Stresses. Appl Sci 2022;12(15):7479. https://doi.org/10.3390/app12157479.

[5] Do D-P, Tran N-T, Mai V-T, Hoxha D, Vu M-N. Time-Dependent Reliability Analysis of Deep Tunnel in the Viscoelastic Burger Rock with Sequential Installation of Liners. Rock Mech Rock Eng 2020;53(3):1259–85. https://doi.org/10.1007/s00603-019-01975-6.

[6] Chuanqi LI, Zaheri M, Ranjbarnia M, Daniel DIAS. Calculating of the tunnel face deformations reinforced by longitudinal fiberglass dowels: From analytical method to artificial intelligence. Transp Geotech 2023;43:101152. https://doi.org/10.1016/j.trgeo.2023.101152.

[7] Fahimifar A, Zareifard MR. A theoretical solution for analysis of tunnels below groundwater considering the hydraulic–mechanical coupling. Tunn Undergr Space Technol 2009;24(6):634–46. https://doi.org/10.1016/j.tust.2009.06.002.

[8] Fahimifar A, Zareifard MR. A new elasto-plastic solution for analysis of underwater tunnels considering strain-dependent permeability. Struct Infrastruct Eng 2014;10 (11):1432–50. https://doi.org/10.1080/15732479.2013.824489.

[9] Fahimifar A, Ghadami H, Ahmadvand M. The influence of seepage and gravitational loads on elastoplastic solution of circular tunnels *Scientia Iranica. Trans A Civ Eng* 2014;21(6):1821.

[10] Fahimifar A, Ghadami H, Ahmadvand M. An elasto-plastic model for underwater tunnels considering seepage body forces and strain-softening behaviour. Eur J Environ Civ Eng 2015;19(2):129–51. https://doi.org/10.1080/19648189.2014.939305.

[11] Fahimifar A, Ghadami H, Ahmadvand M. The ground response curve of underwater tunnels, excavated in a strain-softening rock mass. Geomechanics and Engineering 2015;8(3):323–59. https://doi.org/10.12989/gae.2015.8.3.323.

[12] Fang Q, Zhang D, Zhou P, Wong LNY. Ground reaction curves for deep circular tunnels considering the effect of ground reinforcement. Int J Rock Mech Min Sci 2013;60:401–12. https://doi.org/10.1016/j.ijrmms.2013.01.003.

[13] Giordanella M, Ranjbarnia M, Oreste P, Zaheri M. Study of the systematic fully grouted rock bolts performance in tunnels considering installation condition of bolt head. Geomech Geoeng 2022;17(4):1151–67. https://doi.org/10.1080/17486025.2021.1928761.

[14] Hoek E. Reliability of Hoek-Brown estimates of rock mass properties and their impact on design. Int J Rock Mech Min Sci 1998;35(1):63–8. https://doi.org/10.1016/S0148-9062(97)00314-8.

[15] Hoek E, Marinos P. Predicting tunnel squeezing problems in weak heterogeneous rock masses. Tunnels and tunnelling international 2000;32(11):45–51.

[16] Hoek E, Carranza-Torres C, Corkum B. Hoek-Brown failure criterion-2002 edition. Proceedings of NARMS-Tac 2002;1:267–73.

[17] Huangfu M, Wang M-S, Tan Z-S, Wang X-Y. Analytical solutions for steady seepage into an underwater circular tunnel. Tunn Undergr Space Technol 2010;25(4): 391–6. https://doi.org/10.1016/j.tust.2010.02.002.

[18] Kargar AR, Haghgouei H. An analytical solution for time-dependent stress field of lined circular tunnels using complex potential functions in a stepwise procedure. App Math Model 2020;77:1625–42. https://doi.org/10.1016/j.apm.2019.09.025.

[19] Kolymbas D, Wagner P. Groundwater ingress to tunnels – The exact analytical solution. Tunn Undergr Space Technol 2007;22(1):23–7. https://doi.org/10.1016/j.tust.2006.02.001.
[20] Nomikos P, Rahmannejad R, Sofianos A. Supported Axisymmetric Tunnels Within Linear Viscoelastic Burgers Rocks. Rock Mech Rock Eng 2011;44(5):553–64. https://doi.org/10.1007/s00603-011-0159-0.
[21] Paraskevopoulou C, Diederichs M. Analysis of time-dependent deformation in tunnels using the Convergence-Confinement Method. Tunn Undergr Space Technol 2018;71:62–80. https://doi.org/10.1016/j.tust.2017.07.001.
[22] Quevedo, F. P. d. M., Bernaud, D., & Filho, A. C. (2022). Numerical Analysis of Deep Tunnels in Viscoplastic Rock Mass Considering the Creep and Shrinkage of the Concrete Lining. *Int J Geomech, 22*(4), 04022005. 10.1061/(ASCE)GM.1943-5622.0002282.
[23] Ranjbarnia M, Zarei F, Goudarzy M. Probabilistic Analysis of Bearing Capacity of Square and Strip Foundations on Rock Mass by the Response Surface Methodology. Rock Mech Rock Eng 2023;56(1):343–62. https://doi.org/10.1007/s00603-022-03090-5.
[24] Song F, Wang H, Jiang M. Analytical solutions for lined circular tunnels in viscoelastic rock considering various interface conditions. App Math Model 2018;55:109–30. https://doi.org/10.1016/j.apm.2017.10.031.
[25] Wang HN, Chen XP, Jiang MJ, Song F, Wu L. The analytical predictions on displacement and stress around shallow tunnels subjected to surcharge loadings. Tunn Undergr Space Technol 2018;71:403–27. https://doi.org/10.1016/j.tust.2017.09.015.
[26] Wang HN, Li Y, Ni Q, Utili S, Jiang MJ, Liu F. Analytical Solutions for the Construction of Deeply Buried Circular Tunnels with Two Liners in Rheological Rock. Rock Mech Rock Eng 2013;46(6):1481–98. https://doi.org/10.1007/s00603-012-0362-7.
[27] Wang HN, Utili S, Jiang MJ, He P. Analytical Solutions for Tunnels of Elliptical Cross-Section in Rheological Rock Accounting for Sequential Excavation. Rock Mech Rock Eng 2015;48(5):1997–2029. https://doi.org/10.1007/s00603-014-0685-7.
[28] Wang H, Song F, Zhao T, Jiang M. Solutions for lined circular tunnels sequentially constructed in rheological rock subjected to non-hydrostatic initial stresses. Eur J Environ Civ Eng 2022;26(5):1834–66. https://doi.org/10.1080/19648189.2020.1737576.
[29] Zaheri M, Ranjbarnia M. Ground reaction curve of a circular tunnel considering the effects of the altered zone and the self-weight of the plastic zones. Eur J Environ Civ Eng 2021;1–24. https://doi.org/10.1080/19648189.2021.1877829.
[30] Zaheri M, Ranjbarnia M. Long-Term Analysis of Tunnels in Rheological Rock Masses Considering the Excavation-Damaged Zone. Int J Geomech 2023;23(1):04022266. https://doi.org/10.1061/(ASCE)GM.1943-5622.0002642.
[31] Zaheri M, Ranjbarnia M. Theoretical and numerical analyses of squeezing rock mass around a spherical opening considering the existence of a damaged zone. Amirkabir Journal of Civil Engineering 2023. 10.22060/CEEJ.2022.20529.7452.
[32] Zaheri M, Ranjbarnia M, Dias D. New analytical approach to simulate the longitudinal fiberglass dowels performance installed at the face of a tunnel embedded in weak and weathered rock masses. Comput Geotech 2023;153:105080. https://doi.org/10.1016/j.compgeo.2022.105080.
[33] Zaheri M, Ranjbarnia M, Goudarzy M. Analytical and Numerical Simulations to Predict the Long-Term Behavior of Lined Tunnels Considering Excavation-Induced Damaged Zone. Rock Mech Rock Eng 2022;55(10):5879–904. https://doi.org/10.1007/s00603-022-02962-0.
[34] Zaheri M, Ranjbarnia M, Oreste P. Performance of systematic fully grouted rockbolts and shotcreted layer in circular tunnel under the hydrostatic conditions using 3D finite difference approach. Geomech Geoeng 2021;16(3):198–211. https://doi.org/10.1080/17486025.2019.1648885.
[35] Zaheri M, Ranjbarnia M, Zareifard MR. A theoretical solution to investigate long-term behavior of pressurized tunnels in severe squeezing conditions. Comput Geotech 2023;159:105499. https://doi.org/10.1016/j.compgeo.2023.105499.
[36] Zareifard MR, Fahimifar A. Elastic–brittle–plastic analysis of circular deep underwater cavities in a Mohr-Coulomb rock mass considering seepage forces. Int J Geomech 2015;15(5):04014077. https://doi.org/10.1061/(ASCE)GM.1943-5622.0000400.
[37] Zareifard MR, Fahimifar A. A simplified solution for stresses around lined pressure tunnels considering non-radial symmetrical seepage flow. KSCE J Civ Eng 2016;20(7):2640–54. https://doi.org/10.1007/s12205-016-0105-5.
[38] Zareifard MR, Shekari MR. Comprehensive solutions for underwater tunnels in rock masses with different GSI values considering blast-induced damage zone and seepage forces. App Math Model 2021;96:236–68. https://doi.org/10.1016/j.apm.2021.03.003.
[39] Zeng GS, Wang HN, Jiang MJ. Analytical solutions of noncircular tunnels in viscoelastic semi-infinite ground subjected to surcharge loadings. App Math Model 2022;102:492–510. https://doi.org/10.1016/j.apm.2021.10.010.
[40] Zeng GS, Wang HN, Jiang MJ, Luo LS. Analytical solution of displacement and stress induced by the sequential excavation of noncircular tunnels in viscoelastic rock. Int J Rock Mech Min Sci 2020;134:104429. https://doi.org/10.1016/j.ijrmms.2020.104429.
[41] Zou J, Li S. Theoretical solution for displacement and stress in strain-softening surrounding rock under hydraulic-mechanical coupling. Sci China Technol Sci 2015;58(8):1401–13. https://doi.org/10.1007/s11431-015-5885-1.